A Contact-Point Based Approach for the Analysis of Reactions among Solid Particles

Vishal V. Dalvi, and A. K. Suresh
Dept. of Chemical Engineering, IIT Bombay, Powai, Mumbai 400076, India

DOI 10.1002/aic.12347
Published online September 23, 2010 in Wiley Online Library (wileyonlinelibrary.com).

The contact-point framework,[1] which replaces the picture of continuous contact between the reactants by contact at a finite number of points, has been proposed as a rational one for treating reactions among particulate solids. However, available models suffer from various drawbacks, the main one being that they do not show the right asymptotic behavior for large number of contact points. A model is presented here, that corrects these deficiencies. The results show that the contact-point model approaches particle-continuum behavior whenever the number of contact points exceeds 500. The model predictions have been compared with some data from our previous work on calcia-alumina system in the temperature range 1,150–1,300°C. The model fits the data well, with the fitted values of diffusivity (of calcia through alumina) being of the order of 10^{-16} m^2/s. © 2010 American Institute of Chemical Engineers *AIChE J,* 57: 1329–1338, 2010
Keywords: solid-solid reactions, contact points, Hao-Tanaka model

Introduction

Solid-solid reactions have many important applications such as in cement and metallurgical industries, manufacture of ferrites, semiconductors, ceramics, dry cells, catalysts, etc. Although thus of considerable industrial importance, quantitative treatment of solid-solid reactions has received much less attention than it deserves.[2–4] Most solid-solid reactions have either been studied only empirically or as extensions of fluid-solid reactions from an engineering standpoint. While studies with potential to provide a rational theoretical basis for the analysis of such reactions have often appeared, these suffer from various drawbacks in the current state of their development. In this article, we present an improved model suitable for particulate systems, and test it against experimental data on the calcia-alumina system.

Solid-solid reactions have been generally analyzed with models inspired by the gas-solid literature, such as the shrinking core model. Models due to Jander, Ginstling-Brounshtein (GB) and their extension by Valenci and Carter are extensively used to describe solid-reaction kinetics and belong to this *genre*. Ghoroi and Suresh[3] have recently surveyed the relevant literature; almost all the models assume diffusion of one reactant species (B) through the product zone as the rate-controlling step. The basic premise behind these models is that the particle A in which reaction occurs is completely surrounded by the diffusing phase. The GB model, for example, treats a partially reacted particle of A as having two regions, an inner core of unreacted A and an outer shell of the product, with the second reactant B diffusing through the shell to meet and react with A at the boundary between the two regions. The analytical treatment leads to the following expression between conversion of A (α), and time (t)

$$\left[1-\frac{2}{3}\alpha-(1-\alpha)^{\frac{2}{3}}\right]=2\left(\frac{D_eC_{B0}}{\nu_Br_{A0}^2C_{A0}}\right)t \qquad (1)$$

where ν_B is a stoichiometric factor. The original radius of the particle r_{A0}, is assumed to remain constant through the reaction. While the expression provides a qualitatively satisfactory fit to experimental conversion-time data, the

Correspondence concerning this article should be addressed to A. K. Suresh at aksuresh@iitb.ac.in.

assumption of A being completely surrounded by (a continuum of) B is questionable in the case of solid-solid reactions; it may, at best, be a useful approximation when particles of B are small in comparison to those of A, and many particles of the former surround each particle of the latter, on average. As an alternative, therefore, models have been proposed, which are based on a finite number of points of contact between the reacting particles.

Komatsu[5] was probably the first to propose a contact point-based model for solid-solid reactions. He considered the number of contact points to change with time. The rate of reaction is assumed to be proportional to the number of contact points and inversely proportional to the product zone depth. Using these assumptions he developed the following equation for the relation between conversion α and time

$$\left[1-(1-\alpha)^{\frac{1}{3}}\right]^2=\left[\frac{2k'n(A/B)}{r_{A0}^2}\right]t+\left[\frac{2k'gn(A/B)}{r_{A0}^2(l+1)t_f^l}\right]t^{l+1}$$

where $n(A/B)$ is the number of particles of B that surround a single particle of A. This equation reduces to Jander's model for a constant number of contact points. To find the unreacted volume, the author made some assumptions on the geometry of the reacting entity, which are open to question.

Several years later, Hao and Tanaka[1] proposed a contact point-based model assuming a constant number of contact points between reacting particles. They used an equation developed by Ouchiyama and Tanaka[6,7] to calculate the number of particles of B in contact with a central particle of A in a random packed bed of A and B, as a function of radius ratio R_r, molar ratio R_m, and molar density ratio R_p

$$N_{AB}=\frac{4(1-\varepsilon_A)[2\gamma+R_r+1]^2[2R_r+\gamma(R_r+1)]^2}{\left[3(\gamma+R_r)^2+(\gamma+1)\left(\gamma+R_r^2\right)\right](\gamma+R_r)^2(\gamma+1)} \quad (2)$$

where ε_A is the surface porosity, and $\gamma=\frac{R_pR_r^3}{R_m}$. The species B is assumed to diffuse from the contact points into the particle of A, and react with it at a reaction front. The mathematical treatment approximates the diffusion as being purely radial (with the origin at the contact point), because of which the reaction fronts turn out to be sections of spheres. A quasi-steady state treatment is used to simplify the consideration of diffusion, and approximations are made to keep the geometrical details tractable. The nature of these approximations is such that the errors become the more serious, the smaller the number of contact points. Since one would anyway expect the shrinking core treatments (e.g., GB) to provide a good approximation in the limit of large N_{AB}, it is precisely the situations of small N_{AB} that call out for an alternative modeling framework. There is, thus, a motivation to reexamine the contact point framework.

There are other fundamental issues with the Hao-Tanaka development of the contact point picture. The model does not tend, as it should, toward the particle-continuum models in the limit of large N_{AB}. Also, the time for complete reaction is independent of N_{AB}. These results, which do not accord with intuition, result from the approximations made in the mathematical treatment. It is, therefore, the purpose of this article to start with the physical picture as provided by Hao and Tanaka,[1] but provide a mathematical development that is consistent with the established models in the appropriate asymptotic limits. Finally, the model developed is tested against available data from the literature.

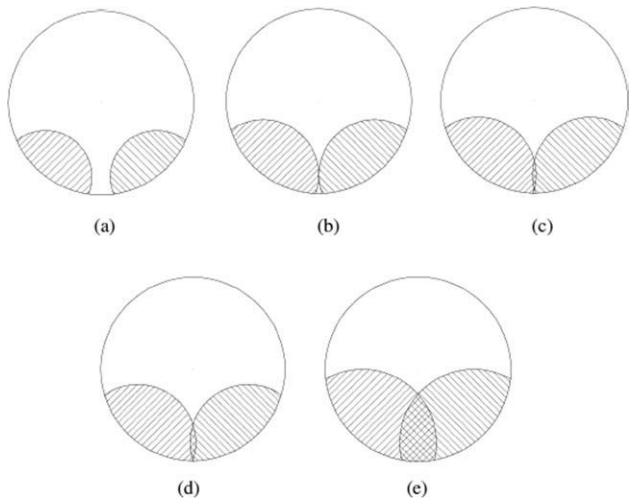

Figure 1. Geometry of the reacting entity at different stages of reaction as conceptualized by Hao and Tanaka.[1]

(a) Phase 1 (transition phase); $\xi < \xi_c$, (b) transition point $\xi = \xi_c$, (c) Phase 2; $\xi_c < \xi < \xi'_c$, (d) end of phase 2; $\xi = \xi'_c$, and (e) Phase 3; $\xi'_c < \xi < r_{A0}$. r_{A0} is the radius of the particle (measured from the particle center), and ξ, the radius of the product zone (shaded region), measured from the contact point.

Hao-Tanaka model

For solid-solid reactions in general, the diffusing component can be identified by experimental techniques (see Hao and Tanaka[8]). Consider a reaction between particles of A and B, with B diffusing into A. Hao and Tanaka[1] divide the time for total conversion of the particle A into three phases (see Figure 1). In the first phase (Figure 1a), the reaction proceeds into the particle from the contact points (modeled as cylindrical disks of thickness ξ_1), with the (non-overlapping) product zones being spherical sections centered at the contact points. This phase (called the transition phase) ends when the neighboring product zones touch (Figure 1b). The time at which this happens is designated as t_c.

In the second phase (Figure 1c), the product zones partially overlap, but there is some unreacted material at the periphery. To deal with this situation, the authors made an assumption that every product zone is surrounded by four other product zones which overlap with it after the transition phase. The second phase ends at time t'_c, when the overlap zone reaches the particle surface. As a further approximation, Hao and Tanaka[1] assume the outer surface to be completely covered by product zones at this stage, and calculate the radius of the product zone at the end of phase 2, on that basis.

In the final phase (Phase 3, Figure 1e), the outer region is completely converted and the unconverted part is confined to a "golf-ball" like core region, which then recedes toward the particle center. The particle is taken to be completely converted when the front radius ξ equals the particle radius.

Several publications from this group[1,2,9] give details of the derivations. The relation between the radius of the reaction front ξ (see Figure 1), and time is given, for all phases, by

$$\xi^3 = \frac{3D\xi_1}{K}t \tag{3}$$

where $K = \frac{b\rho_A}{a\rho_B}$.

At any stage of reaction, reactant conversion is calculated from the total volume of the product zones V, as

$$\alpha_A = \frac{V}{\left(4/3\right)\pi r_{A0}^3} \tag{4}$$

The relation between V and ξ in the different phases is developed from geometric considerations. Details are available in the cited references.

For ease of application, the authors fit the final conversion-time relationship to an Avrami type function

$$\alpha_A = 1 - \exp(-\kappa\tau^\eta)$$

where κ and η are a function of a number of contact points, and $\tau = \frac{t}{t_f}$, t_f, being the time for complete conversion. Hao and Tanaka[1] provide a plot from which κ and η can be found for a given value of N_{AB}.

The time t_f for complete conversion, calculated from Eq. 3 for κ and η, is seen to be independent of the number of contact points. Also, the model does not reduce to the particle-continuum models as the number of contact points increases. The authors claim that the contact point approach is fundamentally different, and is not in any sense a generalization of the particle-continuum class of models. The authors fit their model to some data on Fe_2O_3–V_2O_5 system,[10] and claim it to be superior in that it gives the same value for the rate parameter (diffusivity) for different particle-size ratios in the reactant mixture, while the Ginstling-Brounshtein (GB) model returns different values. However, the number of contact points in these situations is so large (at least 600) that, one would intuitively expect the GB model to hold quite well. One would, therefore, trust the GB estimates, and look elsewhere for an explanation of why the parameters returned depend on the particle radius ratio.

In the following, we develop a model based on the contact-point framework provided by Hao and Tanaka[1], but one that attempts to address the above issues. Furthermore, recognizing that the assumptions on geometry that are admissible in the general case, are not necessarily so for the case of small numbers of points of contact, the latter cases are treated separately and individually.

Model development: General case

Consider a reaction $aA + bB \rightarrow product$ between particles of A and B, with B diffusing into A. We assume no significant change in volume as a result of reaction. We treat the diffusion of B into A from any contact point as one-dimensional (1-D) and radial, and divide the life of the reacting particle into three phases as done by Hao and Tanaka.[1] Strictly speaking, at the end of phase 2 (i.e., at t'_c, see Figure 1d) when the overlap zones extend to the surface, the surface of the particle is not completely covered by the footprints of the product zones as assumed, since the spherical surface cannot be tessellated by circles. There, thus, exists an intermediate phase after t'_c during which the unreacted material at the surface disappears completely. However, the following considerations show that this period is likely to be of short duration in general. These considerations also form the basis for some of the assumptions in geometry in what follows.

The following considerations apply to cases of N_{AB} that are not too small (these cases will be individually considered later). Consider the reacting particle in Phase 1. The assumption of 1-D radial diffusion is, generally speaking, a good approximation in this case. The flux vectors (of B) near the surface do deviate from being purely radial and will have a θ – component (since the flux of B cannot cross the particle surface), but the effect of this would be slight, since it is only the edges of the product zones that are affected. Beyond the transition phase, however, the flux vectors will have a θ– as well as a ϕ– component even in the interior region, although the effect is most apparent in the regions of overlap of product zones. The effect of these (θ – and ϕ –) components will be to "smoothen" the corners of product zones where they intersect and overlap, at rates faster than a purely radial treatment would allow. One consequence of this will be that the interstitial spaces surrounded by the footprints of the product zones on the surface will shrink rapidly, so that the surface of the particle is completely tessellated quickly after the end of phase 2. Another effect will be on the shape of the unreacted core in the center of the sphere. This region, which has fingers extending to the surface between product zones at the start of phase 2, will quickly truncate to a golf ball-like shape as the fingers snap in the middle, and the two bits retract rapidly to convert unreacted A in these regions. The golf ball-like shape itself will tend toward sphericity as the sharp corners get further smoothened out, so that the final stages of reaction might be expected to occur on a spherical reaction front, as in the particle-continuum case.

In order to visualize the aforementioned changes in geometry more concretely, some finite element simulations were carried out[11] in two dimensions using the COMSOL Multiphysics® simulator. In these simulations, the 2-D diffusion-reaction problem in a cylindrical disk of A, surrounded by N_{AB} disks of B, was formulated in the COMSOL environment, and solved with the appropriate boundary conditions. Models of this type, which account for reaction in a finite volume, tend to reaction-at-a-front type of models when the ratio of the rate constant to diffusivity (i.e., the Thiele modulus) is large.[3] The iso-concentration profiles predicted in the COMSOL simulation for such parameter values, at different stages of conversion, were compared with those predicted as in this article, considering only the radial component of diffusion. While full details of these simulations will be reported in a separate publication, Figure 2 shows a typical result for eight contact points, at a point in time that corresponds to phase 3. Clearly, the treatment that considers the full dimensionality of the problem leads to a structure of the core that is much closer to a circle than the radial diffusion approximation.

It is clear that the aforementioned conclusions cannot be generalized in all aspects to cases in which the number of

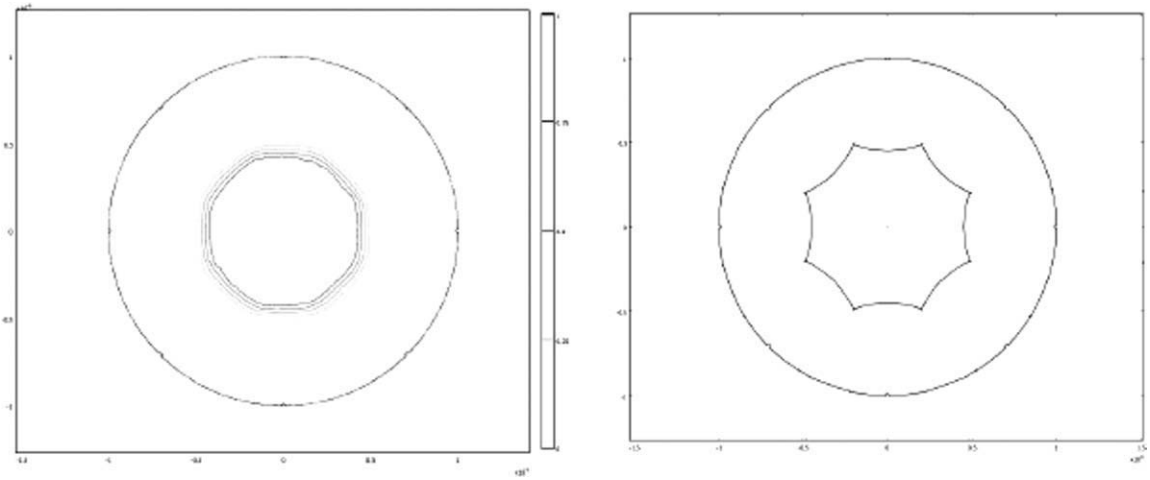

Figure 2. 2-D COMSOL simulation result showing iso-concentration surfaces (left), and its comparison with the contact point treatment (right), assuming purely radial diffusion with diffusion-controlled reaction at the front (parameters used: $r_{A0} = 1 \times 10^{-6}$ m, $N_{AB} = 8$, C_{A0} mol/m^3, $t = 4{,}500$ s).

The profiles shown for the COMSOL simulation are in the region in which a concentration variation of *A* exists.

contact points is very small (e.g., $N_{AB} = 1, 2$, etc.). The model development for these cases will be carried out separately in the next section. In this section, the model development is described for values of N_{AB} that are not too small, with assumptions made in the light of the foregoing discussion.

The model development is carried out in two stages. First, we develop the relation between the front position and time from diffusion considerations. Second, we develop the relation between conversion and the radius of the product zone from considerations of the geometry of the partially reacted particle.

Relation between product zone radius and time

Reactant *B* is assumed to diffuse radially into the particle of *A*, from each contact point, reacting with *A* at a (spherical) front that proceeds into the particle of *A*. Diffusion is treated in a quasi steady state manner. The product zone associated with a single contact point is shown schematically in Figure 3. After Hao and Tanaka,[1] we assume the contact between particles to occur at a disc of thickness ξ_1 (rather than at a point) to be able to treat diffusion.

Equating, for each contact point, the molar rate of diffusion (mol/s) of *B* across the contact disc, that through the product layer at any position *r* and the molar rate of consumption at the reaction front to eliminate intermediate concentrations, we get for the molar rate of *B* uptake of per contact point R_{Bi}, as in Hao and Tanaka[1]

$$R_{Bi} = \frac{\rho_B}{\frac{\xi_1}{S_1 D_P} + \frac{1}{D}\int_{\xi_1}^{\xi} \frac{dr}{S(r)} + \frac{1}{k_r S(\xi)}}$$

where $S(r)$ is the area of a spherical section at any radius *r* within the product zone as shown in Figure 3, and k_r is the surface reaction rate constant. The denominator in the aforementioned equation may be regarded as the total resistance to the diffusion-reaction of *B*, being due to (a) diffusion across the contact disc, (b) diffusion across the product zone, and (c) surface reaction. Assuming product layer diffusion control we get, for the total molar rate of consumption of *B* for N_{AB} contact points

$$R_B = \frac{D\rho_B N_{AB}}{\int_{\xi_1}^{\xi} \frac{dr}{S(r)}} \tag{5}$$

The rate of consumption of component *A* by reaction at the front is related to the rate of movement of front, as

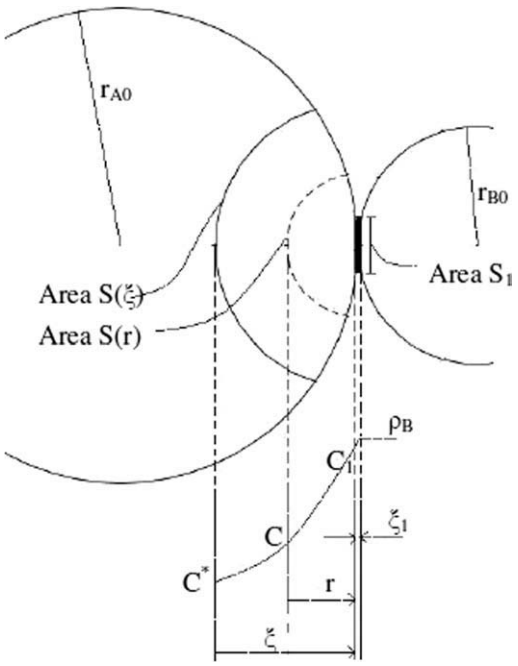

Figure 3. Schematic showing diffusion and development of product zone from a contact point.

$$R_A = N_{AB}\rho_A S(\xi)\frac{d\xi}{dt} \tag{6}$$

Relating the rates of consumption of A and B using the reaction stoichiometry and integrating, we get

$$\int_{\xi_1}^{\xi} S(\bar{\xi})\left[\int_{\xi_1}^{\bar{\xi}} \frac{dr}{S(r)}\right] d\bar{\xi} = \frac{D}{K}t \tag{7}$$

where

$$K = \frac{b\rho_A}{a\rho_B}$$

In order to evaluate Eq. 7 in closed form, Hao and Tanaka[1] assume an inverse proportionality between $S(r)$ and r^2. This allows an elimination of $S(r)$ from Eq. 7 and an analytical integration, leading to Eq. 3. The assumption, however, is strictly valid only if the product zone were to be a cone with the spherical reaction front as the base and the contact point as the apex. In general, therefore, it underestimates $S(r)$, the magnitude of the error increasing as the product zone radius increases, especially for small N_{AB}. We, therefore, prefer to calculate $S(r)$ without this assumption. The equations that govern $S(r)$ depend on the stage of reaction and are shown in Table 1 for ease of reference. Details of derivation are given in the Appendix.

As described earlier, the different phases of particle conversion are demarcated by the positions of the front at the transitions, and these are calculated as in Hao and Tanaka[1] since the definition of the phases are identical in our work and theirs. Thus, the end of phase 2 occurs when

$$\xi = \xi'_c = \frac{2r_{A0}}{\sqrt{N_{AB}}} \tag{8}$$

a result that follows from the Hao-Tanaka assumption that the surface of the reacting particle is completely covered by the footprints of the product zones at this point. Using this result with some geometrical considerations, it is easily shown that the end of phase 1 occurs when

$$\xi = \xi_c = \frac{2r_{A0}}{N_{AB}}\sqrt{N_{AB}-1} \tag{9}$$

Equations 8 and 9 show that the difference between ξ_C and ξ'_C (and, hence, the importance of phase 2) becomes negligible at large values of N_{AB}. In fact, for large N_{AB}, most of the particle gets converted in phase 3.

The integration indicated on the left side in Eq. 7 is carried out as follows. In phase 1 ($0 < t < t_c$ and $\xi_1 < \xi < \xi_C$), we substitute for $S(r)$ (first row of Table 1), and integrate until $t = t_c$. In phase 2, the integral is evaluated in two parts; Eq. 7 is written as

$$\int_{\xi_1}^{\xi_C} S(\bar{\xi})\left[\int_{\xi_1}^{\bar{\xi}} \frac{dr}{S(r)}\right] d\bar{\xi} + \int_{\xi_C}^{\xi} S(\bar{\xi})\left[\int_{\xi_1}^{\bar{\xi}} \frac{dr}{S(r)}\right] d\bar{\xi} = \frac{D}{K}t$$

Table 1. Expressions for the Surface Area $S(r)$ for Moderate and Large N_{AB}. 'p' Stands for the Number of Product Zones That Surround Each Product Zone (See Appendix for Derivation)

Phase	Range of r	Surface area, $S(r)$
1, 2 or 3	$\xi_1 \le r \le \xi_c$	$2\pi r^2\left(1-\frac{r}{2r_{A0}}\right)$
2 or 3	$\xi_c \le r \le \xi'_c$	$2\pi r^2\left[\left(1-\frac{r}{2r_{A0}}\right)-p\left(1-\frac{\xi_c}{r}\right)\right]$
3	$\xi'_C \le r \le r_{A0}$	$2\pi r^2\left(1-\frac{r^2+r_{A0}^2-r_F^2}{2r_{A0}r}\right)$

Recognizing that the first integral on the left is just Dt_c/K, and splitting the integration interval of the inner integral in the second term into two, the equation becomes

$$\int_{\xi_C}^{\xi} S(\bar{\xi})\left[\int_{\xi_1}^{\bar{\xi}} \frac{dr}{S(r)}\right] d\bar{\xi} = \int_{\xi_C}^{\xi} S(\bar{\xi})\left[\int_{\xi_1}^{\xi_C} \frac{dr}{S(r)} + \int_{\xi_C}^{\bar{\xi}} \frac{dr}{S(r)}\right] d\bar{\xi} = \frac{D}{K}(t - t_C)$$

where appropriate expressions from Table 1 are to be used for $S(r)$ in the two integrals within brackets, depending on the range of r.

In similar manner, the $\xi - t$ relation for the third phase ($t > t'_c$; $\xi > \xi'_C$) is evaluated as

$$\int_{\xi}^{\xi} S(\bar{\xi})\left[\int_{\xi_1}^{\xi_C} \frac{dr}{S(r)} + \int_{\xi_C}^{\xi'_C} \frac{dr}{S(r)} + \int_{\xi'_C}^{\bar{\xi}} \frac{dr}{S(r)}\right] d\bar{\xi} = \frac{D}{K}(t - t'_C)$$

with the appropriate expressions for $S(r)$ from Table 1 having to be used in the three integrals within brackets, depending on the range of r.

Conversion as a function of front position

The conversion-ξ relation in our development is the same as obtained by Hao and Tanaka[1] in phases 1 and 2, and is developed from the total volume of all the product zones as in Eq. 4; thus, in phase 1 ($\xi_1 \le \xi \le \xi_C$)

$$\alpha_A = \left(\frac{1}{2}\frac{\xi^3}{r_{A0}^3} - \frac{3}{16}\frac{\xi^4}{r_{A0}^4}\right)N_{AB} \tag{10}$$

and in phase 2 ($\xi_c < \xi < \xi'_c$), if p is the number of product zones that surround each product zone, using Eq. A5 in the Appendix

$$\alpha_A = \left[\frac{1}{2}\frac{\xi^3}{r_{A0}^3} - \frac{3}{16}\frac{\xi^4}{r_{A0}^4}\right]N_{AB} - pN_{AB}\left[2\frac{\xi^3}{r_{A0}^3} - 3\frac{\xi_C\xi^2}{r_{A0}^3} + \frac{\xi_C^3}{r_{A0}^3}\right] \tag{11}$$

As Hao and Tanaka[1] point out, for regular polyhedrons whose vertices are the contact points, the number of angles at each vertex is three, four or five depending on the number

Table 2. Expressions for Reacted Volume for Cases of Small N_{AB}

N_{AB}	ξ_c	ξ_c'	Phase 1	Phase 2
1	$2r_{A0}$	-	$\frac{2}{3}\pi\xi^3 - \frac{\pi}{4}\frac{\xi^4}{r_{A0}}$	Does not exist
2	r_{A0}	$\sqrt{2}r_{A0}$	$\frac{4}{3}\pi\xi^3 - \frac{\pi}{2}\frac{\xi^4}{r_{A0}}$	$2\pi\xi^2 r_{A0} - \frac{\pi}{2}\frac{\xi^4}{r_{A0}} - \frac{2}{3}\pi r_{A0}^3$
3	$\frac{\sqrt{3}}{2}r_{A0}$	$\frac{2}{\sqrt{3}}r_{A0}$	$2\pi\xi^3 - \frac{3\pi}{4}\frac{\xi^4}{r_{A0}}$	$6\pi\xi^2\xi_c - 2\pi\left(\xi^3 + \xi_c^3\right) - \frac{3}{4}\pi\frac{\xi^4}{r_{A0}}$
4	$\sqrt{\frac{2}{3}}r_{A0}$	r_{A0}	$\frac{8}{3}\pi\xi^3 - \pi\frac{\xi^4}{r_{A0}}$	$12\pi\xi^2\xi_c - \frac{16\pi}{3}\xi^3 - 4\pi\xi_c^3 - \pi\frac{\xi^4}{r_{A0}}$

of vertices. On the average a value of four can, therefore, be assumed for p.

In phase 3 ($\xi \geq \xi'_c$) it is convenient to calculate conversion from the *unreacted volume*, which in turn is evaluated from the geometry as described in the Appendix (see Eq. A9); the expression for conversion is

$$\alpha_A = 1 - \frac{1}{\left(4/3\right)\pi r_{A0}^3}\left[\frac{4}{3}\pi\xi_F^3 - V_S N_{AB}\right] \tag{12}$$

Model Development: Case of Small N_{AB}

The geometries that arise in the cases of small N_{AB} (e.g., 1, 2 and 3) can be directly visualized so that a separate treatment is possible in these cases. In comparison to the general case described earlier, (a) the value of p for these cases will be less than 4, and (b) the number of phases will in general be less than 3.

For, $N_{AB} = 1$, the entire particle gets completely converted in phase 1 itself. Such a situation could arise, for example, if particles of A far outnumber those of B. Eq. 7 applies, with the corresponding equation for $S(r)$ from Table 1. The reacted volume, for calculation of conversion using Eq. 4, is given in Table 2.

For $N_{AB} = 2$, the two contact points would be located at opposite poles of the particle of A. The particle gets converted in phases 1 and 2. Phase 1 ends when $\xi = \xi_C = r_{A0}$, at which point the conversion is 62.5%. Unlike in the general case, the particle is not completely converted when the front reaches the center (which happens at ξ_c), as there still remains unconverted material at the periphery. Complete conversion, as well as the end of phase 2, is reached when $\xi = \xi'_C = \sqrt{2}r_{A0}$.$S(r)$. $S(r)$ in phase 1, as well as in phase 2 for $\xi_1 \leq r \leq \xi_C$ is given by the same expressions as in other cases (see Table 1). For $\xi_C \leq r \leq \xi'_C$ in phase 2, however, we have (since $p = 1$)

$$S(r) = 2\pi r^2\left[\frac{\xi_C}{r} - \frac{r}{2r_{A0}}\right].$$

Interestingly for cases of 1 and 2 contact points, the reaction front moves *outward* in the final stages of reaction, the reaction getting completed when the front reaches the *outer* surface.

For $N_{AB} = 3$, the contact points are located in a plane and form the vertices of an equilateral triangle. From the geometry, it is clear that $\xi_C = \frac{\sqrt{3}}{2}r_{A0}$ and Eq. 8 gives $\xi'_C = \frac{2}{\sqrt{3}}r_{A0}$. The reaction front gets split after phase 1 ends, and with the progress of reaction, one of the split fronts proceeds toward the center and the other, toward the outer surface. Table 2 gives the expressions for the volume of the product zone in the two phases, and these equations show that the particle conversion at the end of phase 2 is about 90%. It is not necessary to consider a subsequent phase leading to complete conversion in the realm of this class of solutions, since the geometry is unlikely to be faithfully represented by these models under such conditions. Phase 1 is treated as before, as is the evaluation of $S(r)$ except for $\xi_C \leq r \leq \xi'_C$ in phase 2. For the latter case, we have to use $p = 2$ in the general expression and obtain

$$S(r) = 2\pi r^2\left[\frac{\xi_C}{r} - \frac{r}{r_{A0}} - 1\right]$$

For $N_{AB} = 4$, the contact points are located at the vertices of a regular tetrahedron which is inscribed by the particle surface. Considerations of geometry give $\xi_C = \sqrt{\frac{2}{3}}r_{A0}$ and $\xi_C = r_{A0}$. Once again, most (about 97%) of the conversion occurs in phases 1 and 2, and we do not consider the final stages of conversion. The expression for $S(r)$ in phase 2 is given by

$$S(r) = 2\pi r^2\left[\frac{3\xi_C}{r} - \frac{r}{2r_{A0}} - 2\right]$$

Conversions for the aforementioned cases of small N_{AB} are calculated using Eq. 4, and the expressions for the reacted volumes in different stages of reaction are given in Table 2. We now have the conversion-time relationships for small, moderate and large number of contact points, over the entire conversion range. It will be shown in the sequel that these relationships tend smoothly to the Ginstling-Brounshtein model as the number of contact points increases, unlike the Hao-Tanaka model.

Results and Discussion

Typical conversion-time behavior, as predicted by the model, is shown in Figure 4, for different values of N_{AB}. The parameter values assumed correspond to the experimental data on $BaCO_3 - Fe_2O_3$ used by Hao and Tanaka.[1] A surface porosity $\varepsilon_A = 0.3$ has been assumed in all

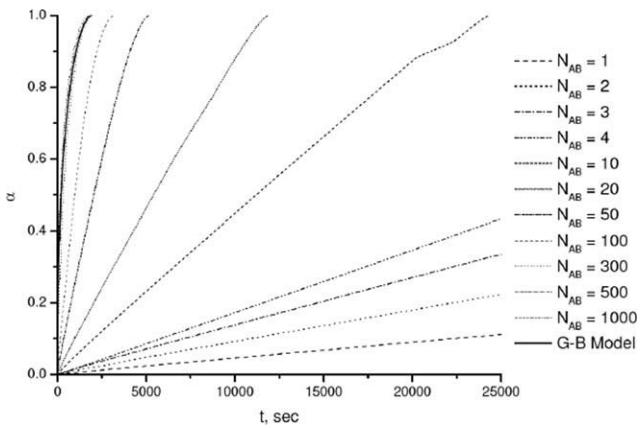

Figure 4. Plot of conversion vs. time for the proposed model for different numbers of contact points $\frac{Kr_{A0}}{D\xi_1} = 1.14\times10^{18}$.

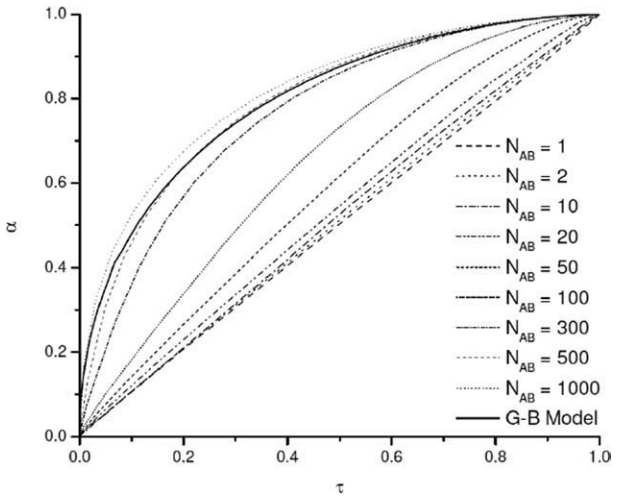

Figure 5. Plot of conversion vs. dimensionless time for the proposed model for different numbers of contact points.

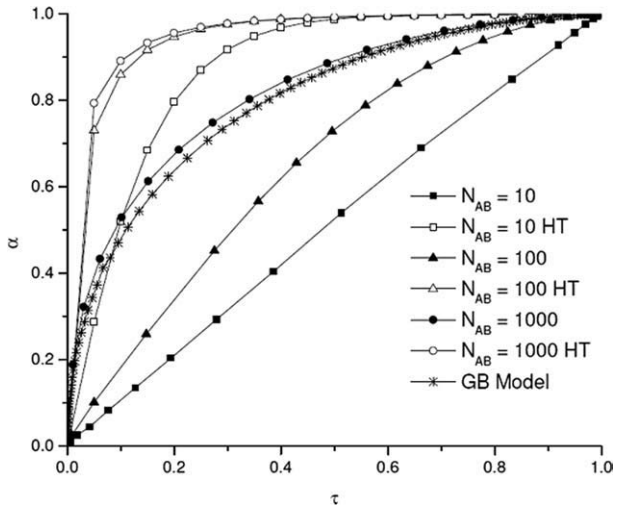

Figure 6. Comparison of the present model, the Hao-Tanaka model and the GB model for conversion-time behavior, for different numbers of contact points.

Filled symbols represent the results from the present model, and open symbols, the corresponding results from the Hao-Tanaka model.

calculations as suggested by Ouchiyama and Tanaka.[6] It is clear that the kinetics depend on the number of contact points for small values of N_{AB}, with the curves coming together for $N_{AB} > 500$. The dependence of the final reaction time on N_{AB} is a noteworthy departure from the behavior of the Hao-Tanaka model. The curve calculated for the GB kinetics is also shown, and it is seen that in the limit of large N_{AB} (> 500), the curves approach GB kinetics, as one would expect. In other words, for, the kinetics would become virtually indistinguishable from particle-continuum kinetics. The conversion-time results for small N_{AB} ($= 1,2,3$ and 4) are also shown in Figure 4, as predicted from the models for these special cases. For reasons that have to do with the neglect of diffusion in the θ– and ϕ– dimensions as discussed earlier, these results would not be expected to be very accurate as conversions tend to 1.

The kinetics can be represented as a function of the single parameter N_{AB} if plotted in terms of the dimensionless time $\tau = \frac{t}{t_f}$, which is the conventional manner in which GB-like kinetics are displayed. Figure 5 shows such a plot. Calculations confirm that beyond values of 1,000, the curves are identical to the one shown for 1,000. The tendency of the model to move toward the particle-continuum (e.g., GB) case is clear. A slight difference between the GB curve and the large N_{AB} (> 500) limit of this model is due to the assumptions in geometry that are made, because of which the core remains nonspherical in this model.

It is seen that, for values of N_{AB} between 1 and 20, the conversion at a given dimensionless time varies linearly with N_{AB}. This fact may be used in interpolating the results for small values of $N_{AB} > 4$, for which analytical results have not been derived.

This model is compared with the Hao-Tanaka model and the GB model in Figure 6. First, as already pointed out, the final reaction time in the latter model is independent of N_{AB}. Second, although a bunching of curves for large N_{AB} is seen, the curves remain different from the GB curve in the limit of large N_{AB}, and in fact move away from it. As pointed out in the introductory section, these features do not accord with expectation. The present model on the other hand, shows a behavior that is intuitively more correct in that, the behavior tends smoothly toward the GB behavior as the number of contact points increases.

It is useful to consider the reasons why this model shows these features while the Hao-Tanaka does not, considering that both start from the same physical picture. A significant point of departure of this development from the Hao-Tanaka model is the manner in which $S(r)$ in Eq. 7 is evaluated in different stages of reaction. Figure 7 shows the ratio $S(r)/S(\xi)$ for a particle which is in phase 3 of reaction, for different values of N_{AB}. The relationship assumed by Hao

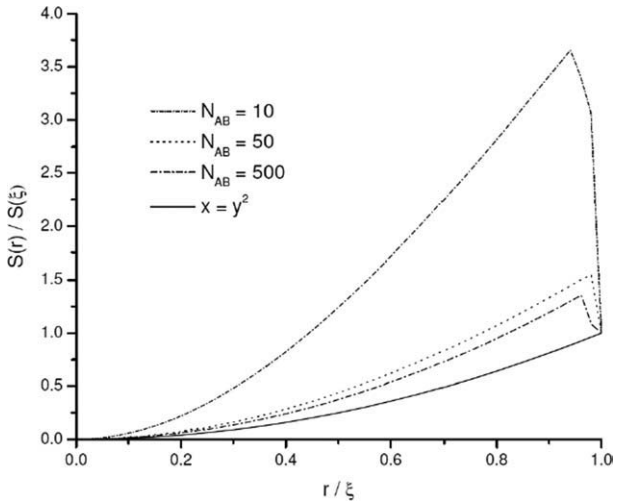

Figure 7. Plot of $S(r)/S(\xi)$ vs. r/ξ for the present model for different numbers of contact points, for a particle which is in Phase 3.

The parabola $x = y^2$ corresponds to the Hao-Tanaka treatment.

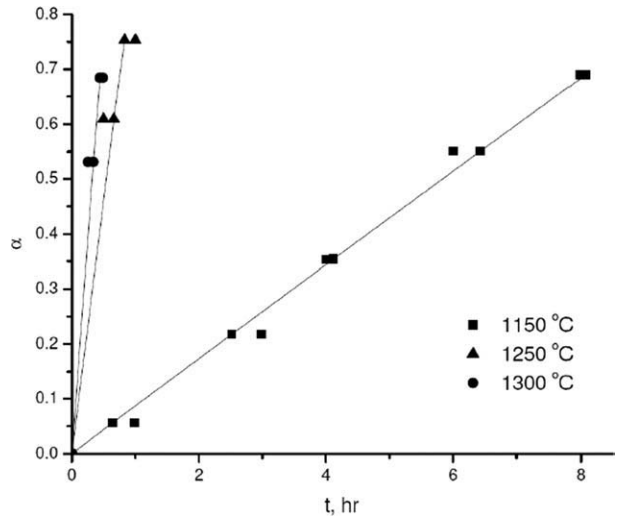

Figure 8. The experimental data of Ghoroi and Suresh[3] fitted with the present model (continuous lines) for NAB = 2.

The estimated values of diffusivity are, respectively, 3.289E-17 m^2/s, 3.579E-16 m^2/s and 6.376E-16 m^2/s at temperatures of 1,150, 1,250 and 1,300°C.

and Tanaka,[1] which allows them to eliminate $S(r)$ in Eq. 7, is also shown for comparison. If the same comparison were to be made in phase 1, the parabolic curve of Hao and Tanaka[1] would agree reasonably well with our results for moderate and large values of N_{AB}. Significant differences arise in phases 2 and 3 of reaction for all values of N_{AB}. These results, in large part, account for the differences in kinetic behavior observed between this development and that of Hao and Tanaka.[1]

Comparison of model with experimental data

Shimizu and Hao[9] attempted a validation of the Hao-Tanaka model with various sets of experimental data from the literature. An examination of the number of contact points estimated by these authors for these data sets reveals that in most cases $N_{AB} > 500$. In view of the observations made earlier, therefore, we would expect the GB model to work well in these cases. We, therefore, need data for smaller values of N_{AB} for verifying the contact point class of models. Ghoroi and Suresh[3] present data for the reaction between $C_{12}A_7(Ca_{12}Al_{14}O_{33})$ and CaO, one of the reactions in the formation of tricalcium aluminate, for which they estimate the number of contact points as 2.3. The conversion data are available at different temperatures.

Figure 8 shows the data of Ghoroi and Suresh,[3] fitted with our model for $N_{AB} = 2$. The parameters for the calculation are taken from the article by Ghoroi and Suresh.[3] Because of the reasons mentioned earlier in the discussion of the model for small N_{AB}, data at large conversions have not been considered in this comparison and only data for $\alpha < 80\%$ have been included. The data are seen to be fitted well. The values of diffusivity at different temperatures, estimated from the fit of the model, are indicated in Figure 8. An activation energy of 378 kJ/mol is calculated for the fitted diffusivities in this work.

It must be noted that estimation of diffusivity from the data using this model requires a value for the thickness of the initial contact disc ξ_1. Shimizu and Hao[9] have used a value of $\xi_1/r_{A0} = 0.05$ after examining data reported for several systems, and the same value has been used here. Ghoroi and Suresh[3] have also used the same value in the fitting of their data with the Hao-Tanaka model. Ghoroi and Suresh[3] have compared their data with several models of the shrinking core *genre*, as well as with the Ishida-Wen model, which is more general in that the reaction is not restricted to the boundary between the shell and the core, in their work. Comparing the values of diffusivity and activation energy they obtain with the present values, we observe that in both cases, these values are higher than what they obtain for the particle-continuum models. The value of activation energy in particular, is higher than what is usually reported in the literature.[3] The literature values, however, are based on GB or Jander models. Clearly, more data are needed (especially over a range of values of N_{AB}) to obtain quantitative values with certainty.

Conclusions

A new model has been developed for the kinetics of solid-solid reactions, within the framework of contact point models. The model shows the right asymptotic behavior in that, as the number of contact points increases, the model approaches the Ginstling-Brounshtein model, which considers the reacting particle to be surrounded by a continuum of the diffusing reactant. In this and other respects, the model is an improvement over the contact-point models in the literature. The cases of very small numbers of contact points have been treated individually since the assumptions to simplify the geometry, made for the general case, do not always apply in such cases, and show a behavior that is qualitatively consistent with that for cases of larger numbers of contact points. The data of Ghoroi and Suresh,[3] on the kinetics of formation of tricalcium aluminate, have been examined in the light of this model. The observed behavior is qualitatively consistent with what is predicted by the model. More experimental data, obtained over conditions of different numbers of contact points, are needed to examine the model critically and obtain parameter values with certainty.

Notation

D = diffusion coefficient of B through the product
K = parameter characteristic of the reaction system, given by Eq. 3
N_{AB} = number of particles surrounding one particle
r = any general radial position within a product zone
t = time for which reaction has been in progress
V = total volume of all the product zones in a particle
X_{VA} = volume fraction of in the initial reaction mixture
ρ = molar density
α = fractional conversion
ε_A = surface porosity
ξ = radius of product zone inside the particle with center at the contact point; position of reaction front
ξ_1 = thickness of the hypothetical small cylinder at the point of contact
ξ_c = radius of product zone at the transition point
D = radius of product zone when surface area of particle is same as that of the product layer.

τ = dimensionless time
γ = ratio of the number of particles of A to that of B
R_r = ratio of the radius of particles of A to that of B
R_ρ = ratio of the (molar) density of A to that of B
R_m = mole ratio of reactants, moles of A to moles of B

Literature Cited

1. Hao YJ, Tanaka T. Analysis of solid-solid reaction controlled by unidirectional diffusion. *Int Chem Eng*. 1990;30:244–253.
2. Ghoroi C, Suresh AK. Solid-solid reaction kinetics - Formation of tricalcium aluminate. *AIChE J*. 2007;53(2):502–513.
3. Ghoroi C and Suresh AK. Intermediate conversion kinetics in tricalcium aluminate formation. *AIChE J*. 2007;53(9):502–513.
4. Suresh AK, Ghoroi C. Solid-solid reactions in series: A modeling and experimental study. *AIChE J*. 2009;55(9):2399–2413.
5. Komatsu W. The kinetic equation of the solid state reaction: the effect of particle size and mixing ratio on the reaction rate in a mixed powder system. *Proc. Fifth Int. Symp. Reactivity of Solids*. Munich, Germany; 1963;182–191.
6. Ouchiyama N, Tanaka T. Estimation of the average number of contacts between randomly mixed solid particles. *Ind Eng Chem Fundam*. 1980;19:338–340.
7. Ouchiyama N, Tanaka T. Porosity of a mass of solid particles having a range of sizes. *Ind Eng Chem Fundam*. 1981;20:66–71.
8. Hao YJ, Tanaka T. A new experimental method to specify the diffusing component in a reacting particulate packing. *Can J Chem Eng*. 1990;68:81–88.
9. Shimizu A, Hao YJ. Influence of particle contact on the estimation of powder reaction kinetics of binary mixtures. *J Am Ceram Soc*. 1997;80:557–568.
10. Shimizu A, Saitou J. Effect of contact points between particles on the reaction rate in the Fe_2O_3-V_2O_5 system. *Solid State Ionics*. 1990;38:261–269.
11. Dalvi VV. *Modeling of Solid-Solid Reactions Based on Concept of Finite Number of Contact Points*. Mumbai, India: IIT Bombay; 2009. Thesis.

Appendix

Calculation of Surface area and volume of product zone in different stages of reaction

Equation 7 provides the relationship between the position ξ of the reaction front and time. To use this relationship, appropriate forms of the function $S(r)$, depending on the stage of reaction, have to be inserted and the indicated integration performed in Eq. 7. Once ξ is calculated, thus, calculation of conversion (Eq. 4) requires a calculation of the total volume of the product zone $V(\xi)$. The details of derivation of $S(r)$ and in different phases of the reaction are given in this appendix.

Phase 1

Figure A1 shows a 2-D cross section of the reacting particle in phase 1, with the product zones from the contact points developing independently. Let r denote some position inside a product zone developing from the contact point P. Assuming diffusion of the species B to be 1-D and radial, the iso-concentration surface at r will be a section of a sphere. Its area can, therefore, be given as

$$S(r) = \psi_1 r^2 \tag{A1}$$

where ψ_1, is the solid angle subtended by the surface at the contact point. Considering the cone with $S(r)$ as the base and apex at A, ψ_1 is related to the apex $2\theta_1$ angle (see Figure A1) as

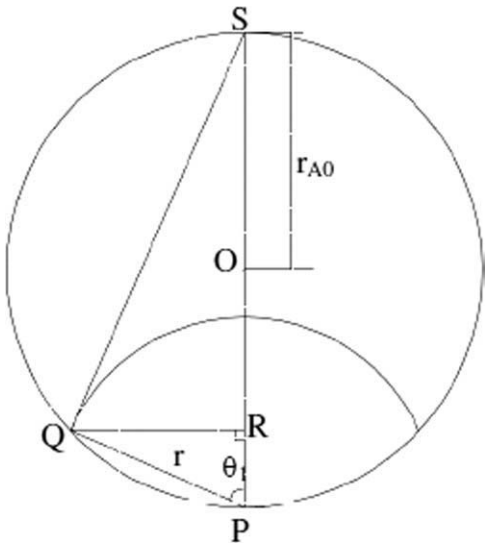

Figure A1. Geometry of the reacting particle in Phase 1.

$$\psi_1 = 2\pi(1 - \cos\theta_1) = 2\pi\left(1 - \frac{r}{2r_{A0}}\right) \tag{A2}$$

since, from triangle ΔPQS

$$\cos\theta_1 = \left(\frac{PQ}{PS}\right) = \left(\frac{r}{2r_{A0}}\right)$$

If the front position (maximum value that r can take) is ξ, Hao and Tanaka[1] show that the total volume of the product zones due to the N_{AB} contact points can be calculated in phase 1 as

$$V = N_{AB}\left(\frac{2}{3}\pi\xi^3 - \frac{\pi}{4}\frac{\xi^4}{r_{A0}}\right) \tag{A3}$$

Phase 2

Figure A2 shows the reacting particle in phase 2. Consider two iso-concentration surfaces from neighboring product zones as shown. If the radius of the surface in question is less than ξ_c, the surfaces do not intersect and the equations of the previous section apply. For $r > \xi_c$ the part of the surface in the overlap region needs to be subtracted. This region is shown in an expanded form in Figure A2 (right). From the geometry

$$\gamma = \cos^{-1}\frac{\xi_c}{r}$$

Using γ to calculate the solid angle subtended by the surface LNM at the contact point P, and, hence, the area of that part of the surface as before, the area $S(r)$ to be considered in the inner integral of Eq. 7 is calculated as

$$a4S(r) = \left[2\pi\left(1 - \frac{r}{2r_{A0}}\right)r^2 - 2\pi p(1 - \cos\gamma)\right] = 2\pi r^2\left[\left(1 - \frac{r}{2r_{A0}}\right) - p\left(1 - \frac{\xi_c}{r}\right)\right] \tag{A4}$$

where p stands for the number of product zones that surround a given product zone.

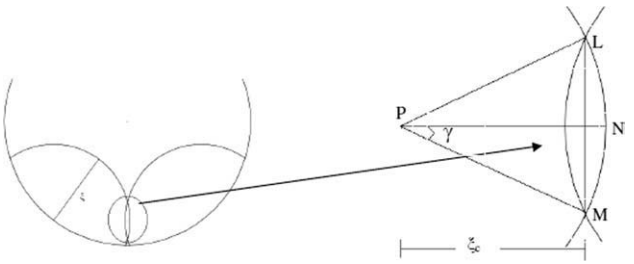

Figure A2. Overlap region in phase 2.

P represents one of the contact points involved.

The volume of the product zone for this case is given by

$$V = \left(\frac{2}{3}\pi\xi^3 - \frac{\pi}{4}\frac{\xi^4}{r_{A0}}\right)N_{AB} - pN_{AB}\frac{V_1}{2} \tag{A5}$$

where V_1 is the overlap volume, shown by Hao and Tanaka[1] to be given by

$$V_1 = \frac{4}{3}\pi\xi^3 - 2\pi\xi_c\xi^2 + \frac{2}{3}\pi\xi_c^3$$

Phase 3

A section through the reacting particle in this phase can be visualized as shown in Figure A3. Considering an iso-concentration surface of radius r in this case, if $r < \xi_c$, $S(r)$ will be given by Eq. A2, and for $\xi_c < r < \xi'_c$, it will be given by Eq. A4. The following considerations apply for $\xi'_C < r < r_{A0}$. From the geometry shown, $S(r)$ for this case is well approximated (the error in the approximation being small because of the 3-D nature of diffusion, as described in the text) by the part of the surface that is included within the sphere of radius r_F where

$$r_F = OF = OH - FH = \sqrt{r_{A0}^2 - \xi_c^2} - \sqrt{r^2 - \xi_c^2} \tag{A6}$$

The point F lies at the apex of the curve of intersection between the two neighboring product zones, and can be solved for, as the intersection of the circle of radius r_F and the circular section representing the product zone centered at P. Taking the contact point P as the origin, and PO as the y-axis, these two curves have the respective equations $x^2 + (y - r_{A0})^2 = r_F^2$ and $x^2 + y^2 = r^2$. Solving these for the y-coordinate y_F of the points of intersection

$$PG = y_F = \frac{r^2 + r_{A0}^2 - r_F^2}{2r_{A0}} \tag{A7}$$

From ΔPFG

$$\theta_2 = \cos^{-1}\frac{PG}{PF} = \cos^{-1}\frac{r^2 + r_{A0}^2 - r_F^2}{2r_{A0}r}$$

and, hence

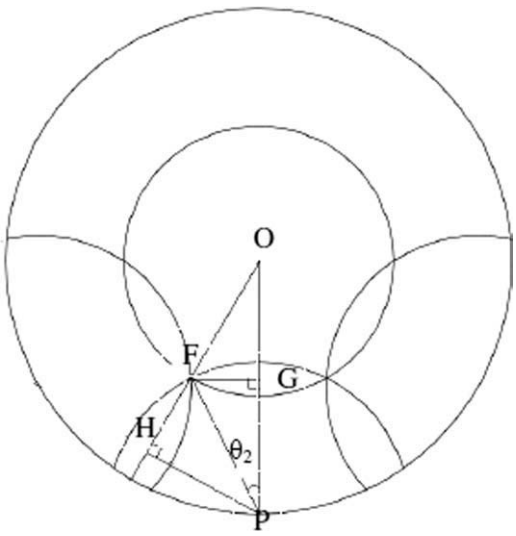

Figure A3. Geometry of the reacting particle in Phase 3.

$$S(r) = 2\pi r^2\left(1 - \frac{r^2 + r_{A0}^2 - r_F^2}{2r_{A0}r}\right) \tag{A8}$$

To calculate conversion, we refer to Figure A3 again, except that the surface of interest now is the surface at $r = \xi$ the position of the reaction front. Denoting the corresponding value of r_F by ξ_F, conversion can be calculated from the volume of the unreacted part, which is largely confined to the structure obtained by subtracting from the sphere of radius ξ_F, the included spherical caps of the product zones. For reasons described in the text (the effect of diffusion in the θ– and ϕ– directions) the error is so approximating is likely to be small for moderate to large number of contact points.

Letting V_s stand for the area to be subtracted due to one contact point, the unreacted volume V_U is given by

$$V_U = \frac{4}{3}\pi\xi_F^3 - V_S N_{AB} \tag{A9}$$

where ξ_F is given by eq. A6 (with r replaced by ξ). Denoting by y_F the y-coordinate of the point corresponding to F in this case, the required volume can be calculated as

$$\begin{aligned} V_S &= \pi\left[\int_{\delta}^{y_F}\left(\xi_F^2 - (y - r_{A0})^2\right)dy + \int_{y_F}^{\xi}\left(\xi^2 - y^2\right)dy\right] \\ &= \pi\left[\left(\xi_F^2 - r_{A0}^2\right)(y_F - \delta) - \frac{1}{3}\left(y_F^3 - \delta^3\right)\right. \\ &\qquad \left. + r_{A0}\left(y_F^2 - \delta^2\right) + \frac{2}{3}\xi^3 - y_F\xi^2 + \frac{1}{3}y_F^3\right] \end{aligned} \tag{A10}$$

where $\delta = r_{A0} - \xi_F$

Manuscript received Jan. 26, 2010, and revision received May 27, 2010.